Numerical Simulation of Welding Quality of Reinforcement Framework Under Different Welding Sequence

Shuwen Ren, Shizhong Chen, Zijin Liu, Zhongxian Xia, Yonghua Wang, and Songhua Li

Abstract The reinforcement framework is welded by the closed stirrup and the main reinforcement. The welding sequence of different welding points on the same stirrup has an important impact on the welding quality of the reinforcement framework. In order to optimize the welding sequence of reinforcement framework, the three-dimensional finite element model of reinforcement framework of six main reinforcement is established to simulate the maximum stress of reinforcement skeleton under three different welding schemes (Scheme 1: welding the upper and lower four welding points first and then welding the middle two welding points; Scheme 2: welding the middle two welding points first and then welding the upper and lower four welding points; Scheme 3: simultaneous welding of six welding points) Residual stress and strain are analyzed and compared to select the best welding scheme. The results show that the residual stress mainly occurs at the solder joint after welding, and the maximum stress value of the solder joint closest to the clamping end is 216.20 MPa. The thermal deformation caused by welding has little effect on the overall size. Compared with Scheme 1 and Scheme 3, the reinforcement framework welded under Scheme 2 has better welding quality.

Keywords Reinforcement framework · Welding sequence · History maximum stress · Residual stress · Strain

1 Introduction

The automatic weld-forming technology of reinforcement framework is a relatively new technology in the forming and processing of reinforcement framework at this

S. Ren · S. Chen · Z. Xia · Y. Wang · S. Li (✉)
School of Mechanical Engineering, Shenyang Jianzhu University, Hunnan District, 25 Hunnan Middle Road, Shenyang, Liaoning 110168, China
e-mail: rick_li2000@163.com

Z. Liu
China Academy of Building Sciences Limited Construction Mechanization Research Branch, 61 Jinguang Road, Guangyang District, Langfang, Hebei 065000, China

stage. Compared with the traditional framework forming and binding technology, it has many advantages, such as lower cost and higher work efficiency, and has gradually become the main processing method of skeleton forming [1, 2]. However, from the point of view of welding technology, the two welded parts to be connected are cylindrical surface with unsmooth surface, and the welding parts are in cross lap state, and the contact area is small, so the solder joint is small, which belongs to special spot welding. During welding, the welding heat effect caused by welding heat source will produce welding thermal stress and thermal deformation, which will affect the welding quality of skeleton to a certain extent. The process maximum stress and welding residual stress will directly affect the tensile and shear properties of the whole skeleton, and the welding thermal strain caused by welding heat will affect the dimensional accuracy of the skeleton to a certain extent [3].

With the continuous development of computer technology, the method of using numerical simulation to predict the residual stress in weldment has been widely used. Xu et al. [4] conducted numerical simulation on the residual stress distribution of CT70 continuous steel pipe under different welding parameters and found that the residual stress of extrusion amount and welding power is inversely proportional, while the welding speed is proportional to the residual stress. Qiao and Han [5] carried out simulation research on different shapes of plates and found that processing the plates into U-shape can significantly reduce the residual stress and strain caused by welding. The relationship between creep failure and residual stress of heat-resistant steel was studied in [6, 7]. It showed that excessive residual stress leads to direct failure of welded parts. However, the research on the stress and strain of steel skeleton in the welding process is still lacking.

Based on the above research, aiming at the improvement requirements of the existing steel framework welding equipment, the equipment transformation is carried out for the situation that the interference phenomenon of each welding joint will appear in the space when six welding points are welded at the same time, and the scheme of batch welding of six welding points on the same stirrup is proposed, and the finite element analysis is carried out. Two improved welding schemes are put forward: For Scheme 1, the upper and lower four solder joints are welded first, and then the middle two solder joints are welded; for Scheme 2, the middle two solder joints are welded first, and then the upper and lower four solder joints are welded; and the original six points simultaneous welding is set as Scheme 3. Through numerical simulation, the overall residual stress and deformation of the reinforced framework after welding under the three schemes can be compared and analyzed, and the optimized processing method is obtained.
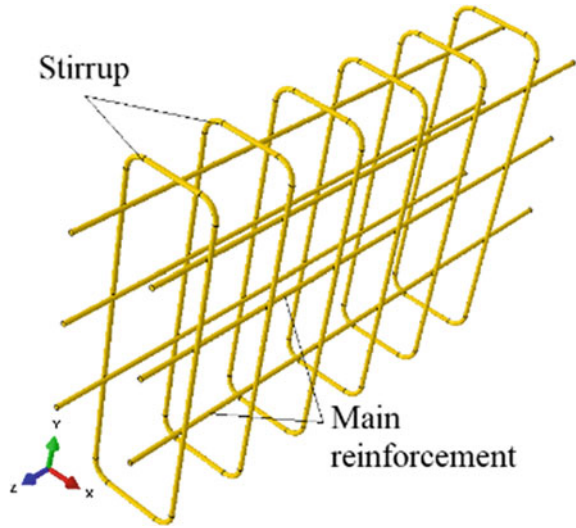
2　Modeling and Simulation Process Design

2.1　Establishment of Finite Element Model

The main components of reinforcement framework are main reinforcement and stirrup. As shown in Fig. 1, in order to adhere to the actual reinforcement framework specification, reduce the simulation calculation process and ensure the reliability of the simulation results, and the framework model is designed to be composed of six main reinforcements with length of 1 m and six stirrups (but only the first five stirrups are welded, and the sixth stirrup is regarded as the observation object), and the stirrup spacing is set as 150 mm. According to the characteristics of the whole structure of the reinforcement framework, the model is divided into 69,333 elements by tetrahedral meshing technology, and the grid independence is verified. Whether the number of elements continues to increase or decrease, the final calculation results are not affected. Therefore, considering the cost, time and accuracy of calculation results, it is appropriate to divide the model into 69,333 units. The meshing of solder joint is shown in Fig. 2.

### 2.2　Establishment of Analysis Step

According to the actual welding situation, the sequential coupling analysis method is adopted, and the subroutine is used to move the input of body heat source. Since the welding method of reinforcement framework is carbon dioxide protection welding,

Fig. 2 Grid division of
solder
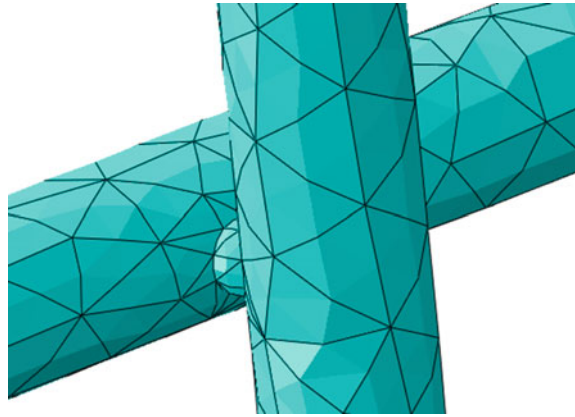
the moving speed of heat source in subprogram should be set as 0 m/s. Due to the limitation of heat source applied by subroutine, only single coordinate point can be input with heat source each time. Therefore, the subprogram is used for the design simulation process to apply body heat source to single solder joint. From the second simulation, the results of the previous simulation are used as the pre-defined temperature field. For the whole welding process, each welding may be 2, 4, or 6 points at the same time. Therefore, when using the last simulation results as the pre-defined temperature field in the same welding step, only one analysis step needs to be set, and the last simulation results are applied to this analysis step as the pre-defined temperature field. If two adjacent simulations of different welding steps are performed, two heat transfer analysis steps need to be set in the first simulation of the next welding step. The results of the previous simulation are applied to the first analysis step as the pre-defined temperature field of the first analysis step, and the setting is not transferred to the second analysis step, and the second analysis step is set as the welding step to be simulated this time. Therefore, for the whole model, a total of 30 times of temperature field simulation analysis are needed, and finally, the temperature field simulation results on the whole reinforcement framework after welding are obtained. After that, a static simulation is carried out. According to the results of temperature field after welding, a static analysis step is set, and full constraints are applied at one end of the six main reinforcements to simulate the clamping of the equipment on one end of the skeleton during welding. The constraint position is shown in Fig. 3. Finally, a static analysis step with a duration of 1 s is set to simulate the state after clamping removal, and the constraints set in the previous step are canceled in the analysis unit [8].

Fig. 3 Clamping force constraint
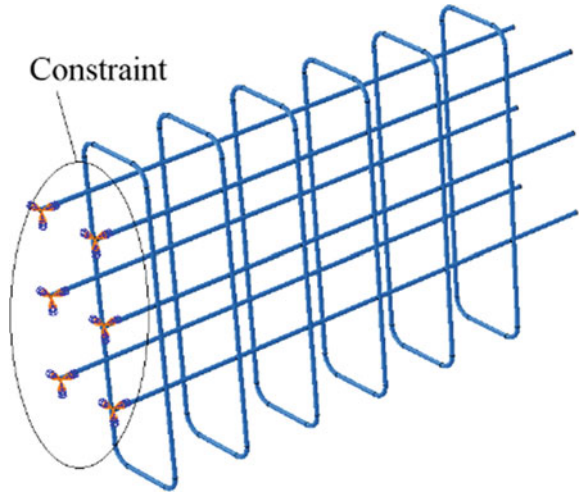
2.3 Heat Input

According to the different input methods of heat source, the heat source can be generally divided into concentrated heat source, plane distribution heat source and volume distribution heat source. CO_2 gas shielded welding is a kind of high-temperature melting electrode produced by the contact between the weldment and the welding wire. After the welding rod melts, it forms molten droplets and enters into the molten pool under the influence of its own gravity and electromagnetic force, so as to fill the welding seam. According to the characteristics of CO_2 gas shielded welding, the fixed-point surface heat source is input to the weldment, so the plane Gaussian distribution heat source is selected as the heat source input form. Heat input is carried out for each solder joint on the model, and the coordinates of different solder joints are set in the subroutine to apply to the corresponding simulation [9]. According to the available data, the heat flux density input formula of moving plane Gaussian heat source is as follows:

$$q(r, x, y, z) = \frac{3\eta U I}{2\pi r^2} \exp\left(-\frac{3(z - vt)^2}{r^2}\right) \tag{1}$$

Because the heat source will not move in the actual welding process, the velocity $v = 0$ m/s; 'r' is the action radius of the heat source, according to the actual measurement, the solder joint radius $r = 6$ mm; '$q(r, x, y, z)$' is the instantaneous heat flux density of any spot; the thermal efficiency can be selected as $\eta = 0.6$; the welding current is $I = 300$ A, the welding voltage is $U = 25$ V; t is the welding time.

2.4 Relationship Between Stress and Strain Caused by Welding Heat

The heating model of cantilever welding is analyzed. The initial welding temperature is T_0 and the length is L_0. When it is heated to raise its temperature to T_1, its length will change to L_1, then the free deformation is ΔL_T:

$$\Delta L_T = L_1 - L_0 = \alpha L_0 (T_1 - T_0) \tag{2}$$

where α is the coefficient of thermal expansion of the material. The free deformation rate ε_T is as follows:

$$\varepsilon_T = \Delta L_T / L_0 = \alpha (T_1 - T_0) \tag{3}$$

However, when the weldment is blocked and cannot be completely deformed, the deformation can only be partially realized, and the part that cannot be shown is internal deformation. According to Hooke's law, the stress and strain in the elastic range meet the linear relationship:

$$\sigma = E\varepsilon = E(\varepsilon_e - \varepsilon_T) \tag{4}$$

2.5 Parameter Setting of Skeleton Material

In the process of finite element analysis, the setting of material parameters is a crucial part, which directly affects the authenticity of simulation results. Especially in the simulation of welding process, the thermal effect of welding process makes the properties of materials change nonlinearly and transiently with the change of temperature. The HRB400 steel bar used in this simulation belongs to low carbon structural steel, and its physical property and mechanical properties can be obtained as shown in Table 1. In addition to setting the material parameters of the skeleton, there are some necessary parameters to be set, such as setting the ambient temperature to 20 °C, the thermal emissivity does not change with the temperature change and is set to 0.7 [10].

Table 1 Material parameters

| Temperature/°C	Thermal conductivity/10^3 W m^{-1} °C^{-1}	Density 10^{-3} Kg m^{-3}	Specific heat capacity J kg^{-1} °C^{-1}	Poisson ratio/μ	Expansivity/10^{-5} °C^{-1}	Elastic modulus/10^5 MPa	Yield stress/MPa
20	0.050	7.80	460	0.28	1.10	2.05	400.0
250	0.047	7.70	480	0.29	1.22	1.87	375.0
750	0.027	7.55	675	0.35	1.48	0.70	280.0
1000	0.030	7.49	670	0.40	1.34	0.20	200.0
1500	0.035	7.35	660	0.45	1.33	0.19	150.0
1700	0.140	7.30	780	0.48	1.32	0.18	120.0

3 Analysis of Simulation Results

3.1 Comparison of Maximum Stress and Residual Stress During Welding Process Under Different Welding Schemes

According to the structural characteristics of the whole skeleton, the maximum stress and residual stress at each point of the skeleton are studied and compared. As shown in Fig. 4, the overall skeleton is ZOY plane symmetric, so only the stress values of points on one side are collected in X direction. After welding, the main stress concentration part of the skeleton should be at each welding point (in the actual welding, the connection failure between stirrup and main reinforcement will occur due to the process maximum stress or excessive residual stress). According to the simulation results, it can be seen that the stress is mainly concentrated at the solder joint, and there is a small stress distribution in the stirrup and other parts of the main reinforcement, as shown in Fig. 5. The solder joint is divided into several grid elements, and the largest maximum history variable unit is collected as the reference point. According to the requirements, collect the solder joints of three main reinforcement and stirrup on one side, a total of 15 points, marking the three main reinforcement as 'a', 'b', and 'c' in sequence, and mark the solder joints on each main reinforcement from left to right as number 1–5 solder joints.

From Fig. 6, it can be concluded that the maximum stress of the three main reinforcements on one side is kept at 40–60 MPa except for number 1 solder joint. The maximum stress is concentrated at number 1 solder joint, and the maximum value is 216.20 MPa. By observing and comparing the characteristics of the values of number 1 solder joint under the three schemes, the historical maximum stress values of number 1 solder joint on main reinforcement 'a' and main reinforcement

Fig. 4 Location and sequence number of acquisition points
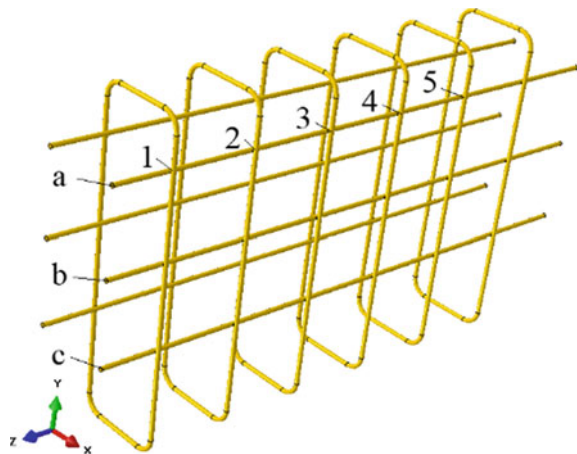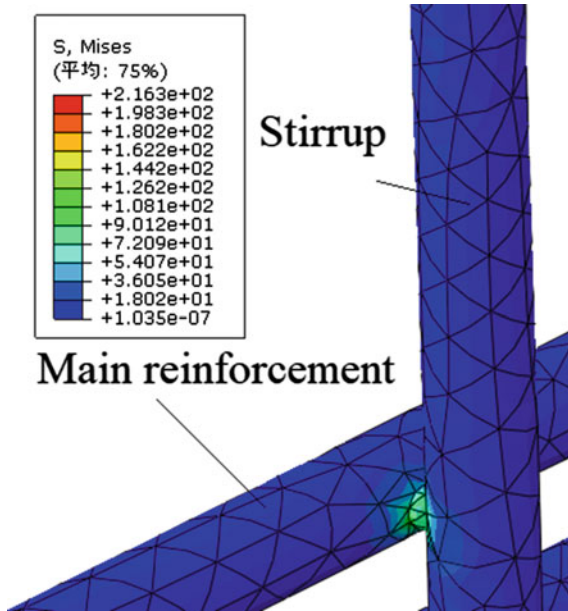
Fig. 5 Residual stress distribution at solder joint

'c' of Scheme 1 and Scheme 3 reach 100 MPa+ and 200 MPa+, respectively, even to the extent that the historical maximum stress values e of number 1 solder joint of main reinforcement 'c' in Scheme 1 is 216.20 MPa, while that of Scheme 2 is only 202.00 MPa on main reinforcement 'b' the historical maximum stress values is the minimum. Therefore, according to the collected historical maximum stress values of each characteristic solder joint, Scheme 2 has the characteristics of optimizing the historical maximum stress values at the solder joint.

The residual stress values of each characteristic solder joint were directly collected 1 s after the constraint was removed, and the following broken line diagram was made.

Observe and analyze the residual stress values of each characteristic solder joint recorded in Fig. 7. Similarly, several solder joints with maximum residual stress are studied and analyzed. In Scheme 1 and Scheme 3, the main reinforcement 'a' and the main reinforcement 'c' have the maximum residual stress at the number 1 solder joint, while, however, in Scheme 2, the maximum residual stress only occurs at the number 1 solder joint of main reinforcement 'b', and its value is smaller than the maximum residual stress 210.2 MPa in Scheme 1 and 201.6 MPa in Scheme 3. Except for a few maximum solder joints, the residual stress of other solder joints in each scheme has little difference, which is less than 30 MPa. Moreover, the number of maximum values in Scheme 2 is less, and the ratio of value to Scheme 1 and Scheme 3 is also lower. According to the analysis of the residual stress at each welding spot, it is shown that the residual stress of the whole skeleton after welding can be significantly improved by adopting Scheme 2.
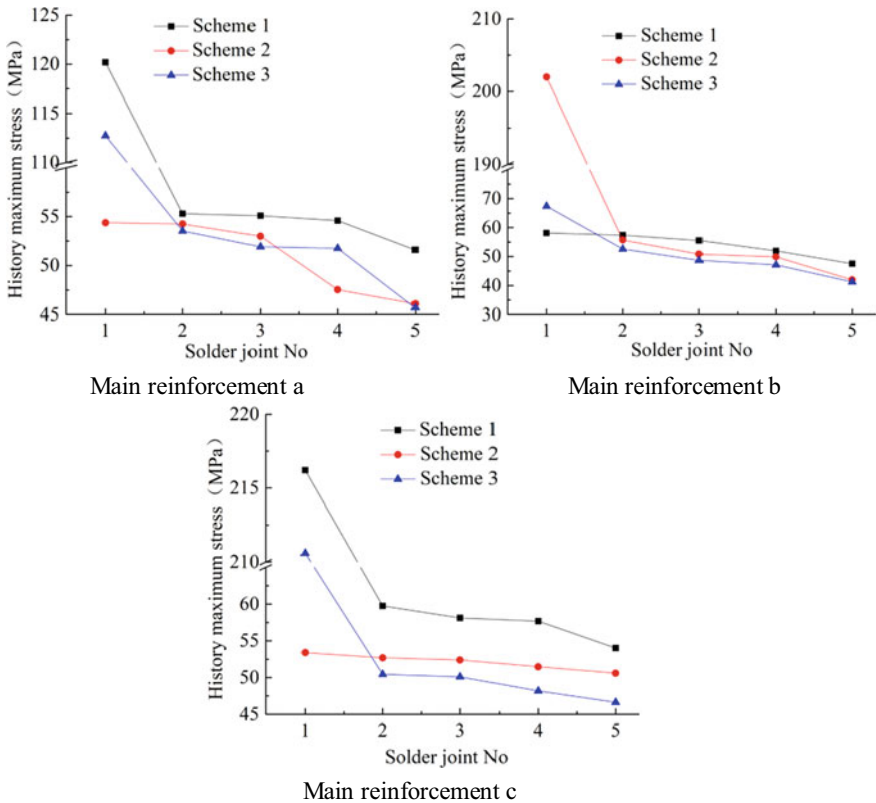
Main reinforcement a

Main reinforcement b

Main reinforcement c

Fig. 6 Comparison of maximum stress of solder joint on main reinforcement under three schemes

3.2 Comparison of Different Strain Under Different Welding Schemes

To study the strain characteristics of the whole skeleton under different schemes, the strain at the maximum strain point of each point on the skeleton is mainly collected. According to the observation of the strain on a single stirrup, 4 characteristic points are collected on one stirrup as the observation points of strain value, as shown in Fig. 8, with a total of 20 recording points. They are numbered according to the sequence from left to right and from top to bottom.

In order to observe the strain of the skeleton at each characteristic point under each scheme, the collected data are made into a broken line chart, as shown in Fig. 9. Compared with the values in Fig. 9, the strain of Scheme 1 is smaller than that of Scheme 2 at each point, especially on the fifth stirrup, the value has a large deviation. It can be seen that the strain of each point in Scheme 2 is the largest. According to the above analysis, a smaller deformation can be obtained by adopting Scheme 1. Therefore, according to the deformation obtained from the simulation, Scheme 1 is
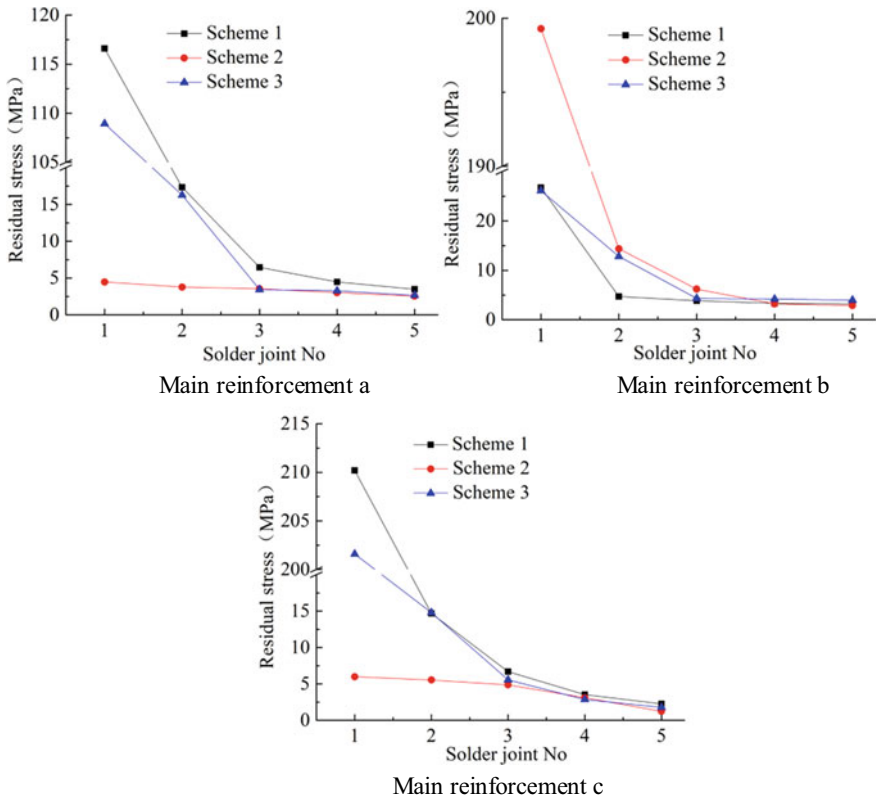
Fig. 7 Comparison of residual stress of solder joint on main reinforcement under three schemes

the better one. This is in contradiction with the results of maximum stress analysis and residual stress analysis.

3.3 Scheme Analysis and Selection

According to the analysis of the maximum stress and residual stress in the course, the quality of the steel frame formed by welding is better under Scheme 2, the welding dangerous points are less, and the residual stress at the welding joint is generally small. However, according to the strain, the overall strain of the welded reinforcement framework is smaller under Scheme 1. However, the quality after welding is comprehensively compared from two aspects of stress and strain, in which the contradiction of large residual stress, small strain and small residual stress and large strain appears. Therefore, it is necessary to continue to analyze the influence of strain characteristics and stress on the quality of the overall skeleton, determine the primary and
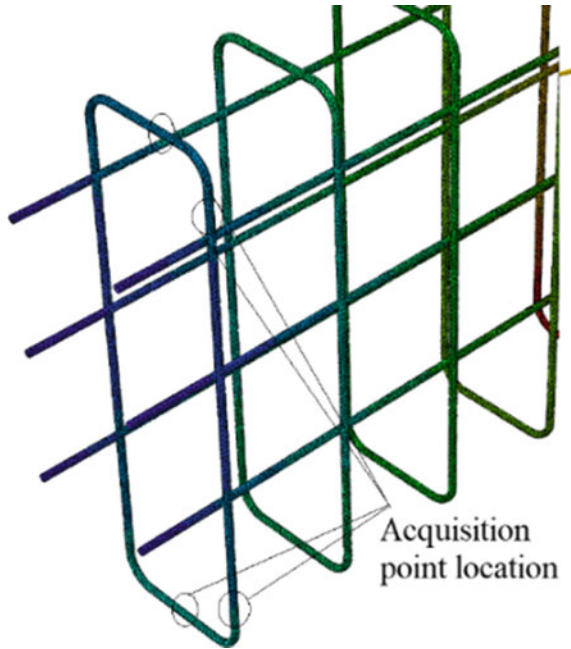
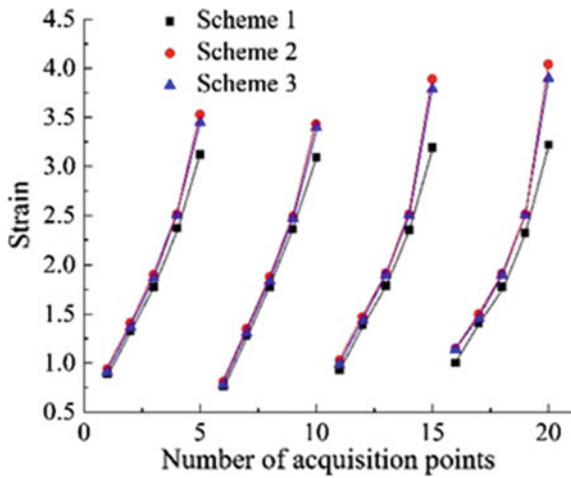**Fig. 8** Location mark of collection point on single stirrup

Fig. 9 Strain of each acquisition point

Table 2 Strain extremum under each scheme

Extremum program	$U1_{\text{Max,Min}}$/(mm)	$U2_{\text{Max,Min}}$/(mm)	$U3_{\text{Max,Min}}$/(mm)
Scheme 1	0.21, −0.17	0.95, −0.10	0.60, −3.50
Scheme 2	0.19, −0.15	1.12, −0.10	0.30, −3.90
Scheme 3	0.29, −0.25	1.01, −0.10	0.64, −3.80

secondary relationship, and then select the scheme. The strain characteristics were further analyzed, and the extreme values of skeleton strain components under each scheme were collected, as shown in Table 2.

From the analysis of the data in the table, the size of each strain component in each scheme shows $\Delta X < \Delta Y < \Delta Z$, and the strain in X direction and Y direction determines the change of cross-sectional area of skeleton. The change in X direction shows that the deformation of Scheme 1 and Scheme 2 is smaller than that of Scheme 3, and Scheme 2 is the smallest; the change in Y direction shows that the deformation of Scheme 1 is smaller than that of Scheme 2; the main strain occurs in Z direction, and the strain difference of three schemes is very small compared with that of Scheme 3, which can be ignored.

In Y direction, the difference of strain between Scheme 1 and Scheme 2 is 0.17 mm, and the overall length of the skeleton is 1 m. Therefore, for the skeleton of general length, the difference is the minimum, which has little impact on the overall quality of the skeleton compared with the residual stress of 100 MPa. Therefore, Scheme 2 is selected as the optimal scheme for welding.

3.4 Analysis and Discussion

According to the analysis results, there are many large residual stresses at the number 1 solder joint in each scheme. Therefore, the number 1 solder joint on the main reinforcement 'a' in Scheme 1 is selected as the research point, and the historical stress curve here is extracted. As shown in Fig. 10, the stress value of all the welding joints on the stirrup where number 1 solder joint is welded is up to 76.21 MPa. The value of the later stage is still increasing, which indicates that the heat input of the later welding also has an effect on the stress value of the solder joint. Moreover, the stress value of number 1 solder joint is much larger than that of the later solder joint due to its very close distance to the clamping point, which indicates that the near-point clamping results in greater stress. According to this phenomenon, a scheme can be put forward. In the welding of the overall main reinforcement framework, the first stirrup welded is designed as the preset stirrup, and it is removed from the overall skeleton after welding. In this way, there will be no extremely dangerous parts in the reinforcement skeleton, so as to ensure the quality of the whole skeleton.

Fig. 10 Stress extraction
value at number 1 solder
joint
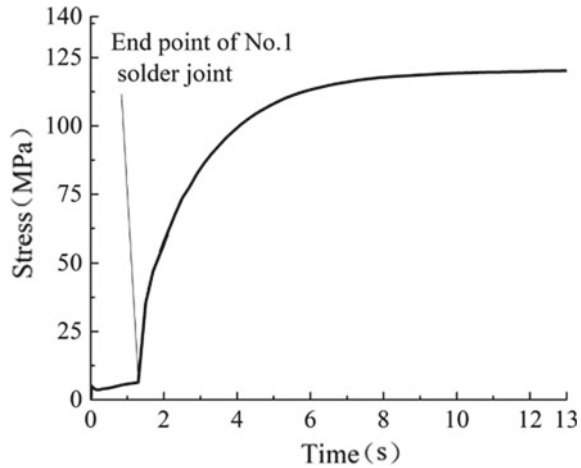
4 Conclusion

In this paper, the welding quality of reinforcement framework under three different
welding sequences are numerical analyzed and discussed, and the following
conclusions are drawn:

1. In the welding process, the welding spot and nearby heat affected zone appear
larger stress, and the stress of base metal is smaller;

2. In the welding process of reinforcement framework, the welding spot on the first
stirrup formed by welding has great welding residual stress. Therefore, the first stirrup
in the reinforcement skeleton belongs to extremely dangerous type, the maximum
residual stress can reach more than 200 MPa after welding, and the mechanical
properties of steel bars in other parts are very poor;

3. In the welding process of reinforcement framework, the main direction of
skeleton deformation occurs in its length direction (i.e., Z direction of this simu-
lation). There is also a small amount of strain on the cross-section, which mainly
occurs in the parallel direction of the side with more stirrups (i.e., the Y direction in
this simulation process);

4. Through the comparison of the maximum stress and residual stress of the three
schemes, it is found that the residual stress of the welded joints of the reinforcement
skeleton is smaller than that of the first scheme, but the difference is smaller than
that of the overall skeleton size, and the influence can be ignored. Therefore, in the
comparison with the three schemes, Scheme 2 is selected as the optimal welding
scheme.

References

1. Chen, B.: The Automatic Control Technology of Forming and Welding for Reinforcing Cage Welding Machine. Changchun University of Technology (2018).
2. Liu, H., Sydora, C., Altaf, M.S., et al.: Towards sustainable construction: BIM-enabled design and planning of roof sheathing installation for prefabricated buildings. J. Cleaner Prod. **235**, 2289–1201 (2019)
3. Knoedel, P., Gkatzogiannis, S., Ummenhofer, T.: Practical aspects of welding residual stress simulation. J. Constr. Steel Res. **132**, 83–96 (2017)
4. Xu, Z., You, Q., Wang, Y., et al.: Numerical simulation of residual stress distribution of CT70 coiled tubing welded by high frequency resistance welding under different welding parameters. J. Netshape Forming Eng. **12**(1), 66–74 (2020)
5. Qiao, L., Han, T.: Effect of geometric shape of plate on residual stress and deformation distribution for butt-weld joint. China Welding **27**(3), 20–26 (2018)
6. Ni, Y., Xu, H., Chang, Y., et al.: Research on elastic-plastic creep damage of notched P92 steel specimens. Mater. High Temp. **35**(4), 335–342 (2018)
7. Zhang, J., Zhang, G., Guo, J.: Numerical simulation on interfacial creep failure of dissimilar metal welded joint between HR3C and T91 heat-resistant steel. J. Wuhan Univ. Technol.-Mate **31**(5), 1068–1074 (2016)
8. Mondal, A.K., Biswas, P., Bag, S.: Experimental and FE analysis of submerged arc weld induced residual stress and angular deformation of single and double sided fillet welded joint. Int. J. Steel Struct. **17**(1), 9–18 (2020)
9. Wang, P., Liu, Y., Chang, H., et al.: Brief analyses of thermo-mechanical coupling issue on welding structures. Trans. China Welding Inst. **40**(7), 006–011 (2019)
10. Jiang, W., Xu, X.P., Gong, J.M., et al.: Influence of repair length on residual stress in the repair weld of a clad plate. Nucl. Eng. Des. **246**, 211–219 (2012)